

# The effect of processing conditions on the microstructure and impact behavior of melt infiltrated Al/SiCp composites

A.M. Zahedi<sup>a</sup>, J. Javadpour<sup>a</sup>, H.R. Rezaie<sup>a</sup>, Mehdi Mazaheri<sup>b,\*</sup>

<sup>a</sup> School of Materials and Metallurgical Engineering, Iran University of Science and Technology (IUST), Tehran, Iran

<sup>b</sup> Laboratory of Complex Matter Physics (LPMC), Ecole Polytechnique Fédérale de Lausanne (EPFL), CH-1015 Lausanne, Switzerland

Received 14 November 2010; received in revised form 14 February 2011; accepted 6 April 2011

Available online 31 May 2011

## Abstract

In the current research, pressureless melt infiltration (PMI) was applied to study the effect of different processing conditions on the final properties of Al/SiC composites, fabricated through the infiltration of aluminum melt into SiC particulates porous preforms. Charpy impact test was used to explore the impact behavior of the Al/SiC composites, obtained from variable processing conditions. Conducting the process at a higher infiltration temperature (1350 °C) increased the final relative density of composites up to the value of 0.97 of theoretical density (TD). The application of a post sintering procedure in nitrogen atmosphere after the completion of infiltration resulted in a slight increase ( $\sim 1$ ) in the final density of composites compared to the only infiltrated ones. Instead, the final density of argon sintered composites has undergone a 0.41% reduction. This can be originated from the occurrence of chemical reactions in the N<sub>2</sub> atmosphere resulting in the formation of consequent phases, contrary to the argon neutral gas. Results concerning with the impact resistance demonstrated a remarkable superiority for the impact energy of the composites subjected to the combined infiltration and sintering (MIS) procedure compared to the infiltrated ones. While such an observation was found to be identical through sintering in both atmospheres, the appearance of brittle phases formed through sintering procedure in nitrogen gave rise to higher impact energy for the argon sintered composites.

© 2011 Elsevier Ltd and Techna Group S.r.l. All rights reserved.

**Keywords:** Composite; Melt infiltration; Preform; Density

## 1. Introduction

The remarkable focus on the hybrid composites, through the recent decade is originated from the combined effects of metallic and ceramic materials relative to the corresponding monolithic alloy. Remarkable properties of these composites such as high strength and modulus accompanied with the excellent high temperature resistance represent these materials as appropriate candidates for automotive and aerospace applications [1–3].

Aluminum composites based on SiC preforms are among the most reputed composites, with a considerable efficiency in the fields of technology due to their high modulus, high specific stiffness, low thermal expansion coefficient, good workability and wear resistance [4–6]. In addition to the numerous methods

initiated to fabricate Al/SiC composites like stir casting, powder metallurgy and pressure melt infiltration [7–10], conducting the process without any external pressure has, recently, appeared as an economic technique, called pressureless melt infiltration [1,11,12]. This process, however, involves some technical obstacles, the most significant of which include formation of an oxide layer on the surface of Al melt during the process and, consequently, poor wetting of the SiC substrate by molten aluminum. The occurrence of undesirable reactions at the Al/SiC interface is another problem, that exerts some variations to the chemical composition of the molten aluminum and this leads to the formation of spam phases at the interface, such as Al<sub>4</sub>C<sub>3</sub> and Al<sub>3</sub>SiC<sub>4</sub> [12]. Pech-Canul et al. [1,11] believe that optimum conditions are to be provided in order that a successful infiltration may be accomplished without any external pressure. Adding preferably more than 3% magnesium to the aluminum melt as well as changing the internal atmosphere of the furnace to 100% nitrogen [11] are among the most significant conditions to ease the infiltration process. Presence of an excellent surfactant such as magnesium allows

\* Corresponding author.

E-mail addresses: [mehdi.mazaheri@epfl.ch](mailto:mehdi.mazaheri@epfl.ch), [mmazaheri@gmail.com](mailto:mmazaheri@gmail.com) (M. Mazaheri).

straightforward removal of oxygen from the melt surface and forms the  $\text{MgAl}_2\text{O}_4$  spinel at the Al/SiC interface. In addition to increasing the driving force for wetting, the reaction of producing  $\text{MgAl}_2\text{O}_4$  spinel consumes the oxygen present in the atmosphere, thins the oxide layer, and thus enhances wetting [13,14]. Besides, application of nitrogen atmosphere not only hinders formation of the oxide layer, but also enhances wetting of SiC by Al melt [11]. Lee et al. [15] conducted the infiltration process under nitrogen atmosphere for an hour, and then cooled it down; again in the flowing nitrogen gas to prevent oxidation. In another research, Zulfia and Hand [4], indicated that the application of  $\text{N}_2$  gas in the infiltration chamber could be effective on the formation of an intermediate magnesium nitride phase, the reaction of which with the Al melt in the forward steps has resulted to the AlN formation, i.e. a reaction with a contributive effect on the whole infiltration kinetics.

On the other hand, combined melt infiltration and sintering (MIS) method has been, recently, initiated to manufacture composites with a high tensile ductility and the probability to attain ductile-phase-toughened composites. As some of the available investigations [16–19] in the literature have alleged, one can observe  $\text{Ni}_3\text{Al}/\text{TiC}$  composites with an enhanced potential structural and wear applications, in case of utilizing this technique. The MIS method, besides, provides high-density materials with an extended compositional range for the tough reinforcing phase. Reports concerning the production of  $\text{Ni}_3\text{Al}/\text{TiC}$  as well as  $\text{FeAl}/\text{TiC}$  composites are available in the literature [20–22]. Plucknett and Becher [23], studied melt infiltration, sintering, and grain growth behavior of MIS-processed  $\text{Ni}_3\text{Al}/\text{TiC}$  composites. They developed a densified  $\text{Ni}_3\text{Al}$ -toughened composite with a homogeneous microstructure in which the tough phase contents vary over the range of 4–25 vol.% [23].

In the present work, however, bearing in mind that composites include higher volume fractions of the aluminum (60 vol.%) as a tough phase, the competence within the MIS technique has been examined through the application of variable processing conditions of final composite.

## 2. Experimental procedure

The silicon carbide (SiC) powder (Carborex, Germany), used in the current investigation, was purchased with the mean particle size of  $90\ \mu\text{m}$ . The SiC powder mixed with 5 wt.% molten paraffin as the binder was initially cold pressed to the green pellets of SiC, under the range of 100–700 MPa, followed by a moderate heat treatment at  $300\ ^\circ\text{C}$  for 30 min to remove the paraffin binder off the green compacts. The specimens were, subsequently, sintered at  $1350\ ^\circ\text{C}$  for 3 h to produce the SiC preforms with the initial density of (density before the infiltration process) 0.4, 0.5, and 0.6 of theoretical density (TD). Due to the weakness of the green compacts, density assessment was only conducted on the sintered specimens and the wide range of compacting pressure was to determine the pressures at which specimens with the closest density value to 0.4, 0.5, and 0.6 TD were attainable after sintering. Note that infiltration procedure has been carried out based on the sintered

preforms with a definite amount of porosity indicated by sintered density of preforms. Thus, green density assessment has not been an influential factor on the output of the current work. The SiC powder as well as the SiC preforms (0.5 TD) and the sintering-compaction behavior of the powder can be seen in Fig. 1(a)–(c), respectively. The SEM micrograph of the SiC preform (Fig. 1(b)), conspicuously, demonstrates the open network of pores for the fluidity of Al melt through the voids of ceramic porous body. The aluminum parts were additionally, supplied from the Al–3 wt.% Mg alloy, the chemical composition of which is embedded in Table 1. Infiltration of the Al melt into the pores of the SiC preforms was carried out in a tube furnace with the nitrogen atmosphere, under a residual pressure of  $0.01333\ \text{Pa}$  ( $10^{-4}$  Torr). Details of the applied raw materials, preform preparation and infiltration procedure can be found in [24]. The experiments included four different procedures with the variable characteristics detailed in Table 2. The higher infiltration temperature in the MI2 procedure ( $1350\ ^\circ\text{C}$ ) demonstrated the influence of temperature on the development of the infiltration process and consequently on the value of impact energy. The application of a combined melt infiltration and sintering (MIS) method was examined through the instigation of MIS1 and MIS2 procedures, the sintering stage of which was performed in the argon and nitrogen ambient, respectively. Designing three sintering temperatures of 1150, 1250, and  $1350\ ^\circ\text{C}$  for the three firing regimes of MIS2 procedure was to make sure about the relevance between the presence of nitrogen and infiltration development by varying

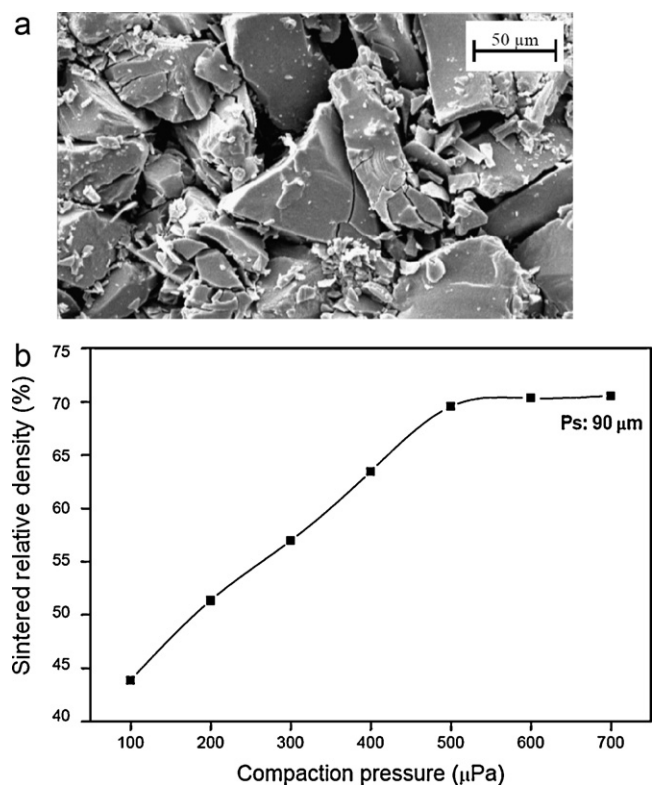


Fig. 1. Scanning electron micrograph (SEM) of (a) SiC powder with mean particle size of  $90\ \mu\text{m}$  and (b) SiC porous preform. (c) Sintered relative density of the SiC powder as a function of the compaction pressure.

Table 1  
Chemical analysis (wt.%) of the applied Al–3 wt.% Mg alloy.

Al	Mg	Ti	Mn	Cu	Ni	Fe	Si	Zn	Cr
97	3	0.01	0.04	0.008	0.005	0.09	0.07	0.01	0.01

the sintering temperature and thus, the amount of nitrogen in the furnace.

Density assessments of composites were performed after the mechanical polishing of the specimens up to 1 mm from all sides of the pellets, using the Archimedes method. Based on the rule of mixture, theoretical density of composites with 0.4, 0.5, and 0.6 TD initial density was determined to be 2.93, 2.98, and 3.04 g cm<sup>-3</sup>, respectively. What should be taken into account is that the voids in the SiC preforms would be, theoretically, filled by the molten aluminum after the infiltration procedure and as mentioned in the previous paper [24], the initial density of SiC preforms before the infiltration process can be regarded as the volume fraction of the SiC phase in the final composite. Therefore, the volume fractions of the Al and SiC phase in the composite fabricated based on the 0.4 TD preform are near 60 and 40 vol.%, respectively. In order to have visual inference of the constituents, Fig. 2 exhibits microstructure of a melt infiltrated Al/SiC composite fabricated based on 0.5 TD initial preforms, in which the volume fraction the SiC phase (darker phase) has been calculated to be closed to 50 vol.%, using Clemex software. For each data point at least five samples have been tested. To study microstructural evolution of the processed composites with the scanning electron microscopy (SEM, Philips XL30, the Netherlands), the specimens were cut into pieces and the cross section was mechanically polished. Phase characterization of the ultimate composites was performed using the X-ray diffraction (XRD) analysis (Philips, X'Pert, Netherlands). Chemical composition of the specimens was investigated using energy dispersion spectroscopy (EDS) analysis (Philips XL30, the Netherlands). The impact resistance energy of composites was determined using Charpy test based on the application of ASTM, E23. The specimens obtained from compacting the abovementioned powder mixture were subjected to the aforementioned pre-sintering procedure to remove the paraffin binder and subsequently, sintered to derive preforms with the closest initial density values to 0.4, 0.5, and 0.6 TD. The SiC preforms were, afterwards, exposed to the procedures mentioned in Table 2. Details of the experiments pertaining impact energy of composites can be found in [24].

Table 2  
Details of processing conditions for fabrication of the specimens.

Procedure	Infiltration	Sintering
MI1	At 950 °C for 105 min in N <sub>2</sub>	–
MI2	At 1350 °C for 105 min in N <sub>2</sub>	–
MIS1	At 950 °C for 105 min in N <sub>2</sub>	At 1350 °C for 180 min in Ar
MIS2	At 950 °C for 105 min in N <sub>2</sub>	At 1150, 1250 and 1350 °C for 180 min in N <sub>2</sub>

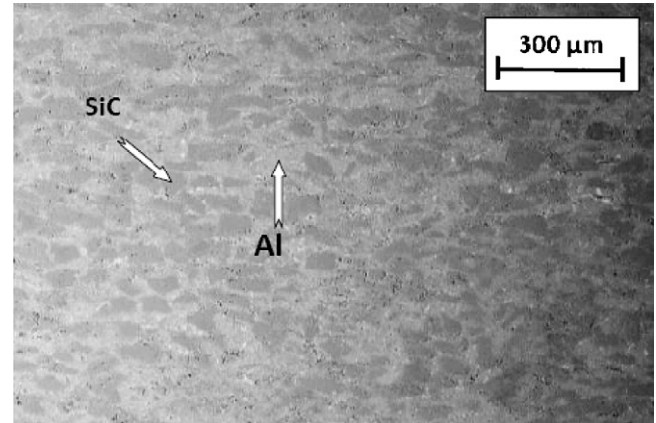


Fig. 2. Scanning electron micrograph (SEM) of the specimen with Al (light phase) and SiC (dark phase) volume fractions of near 50%.

### 3. Results and discussion

#### 3.1. Infiltration and final density of composites

The significant factor influencing on the relative density of melt infiltrated composites is the processing condition in which the infiltration process has been conducted. Therefore, in order to shed light on the characteristics of infiltration trend in different processing regimes, final density of composites have been compared as an assessment tool in this regard.

##### 3.1.1. MI1, MI2, and MIS1

Final density of composites (90 μm, 0.4 TD) fabricated by the MI2 and MIS1 procedures are compared with those obtained from MI1 process, in Fig. 3. As can be observed, application of a higher infiltration temperature in MI2 process has increased the final density of composites to 0.97 TD. Such an improvement compared to the MI1 composites lies in the effective role of temperature to increase Al melt fluidity and reactivity and therefore, to ease the movement of melt through the open pores of SiC preforms [6,24]. As discussed in the literature, the final density improvement resulted from the

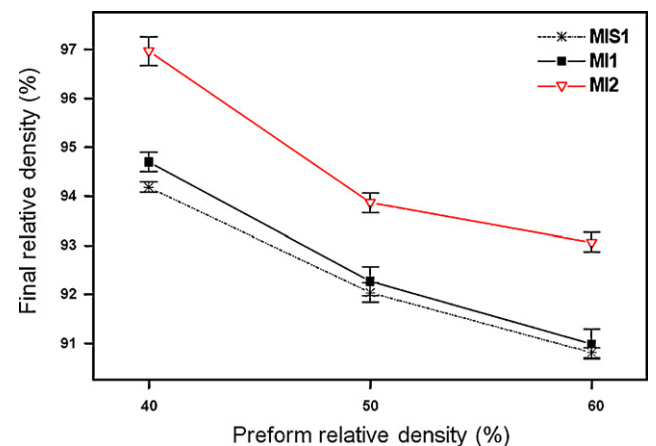


Fig. 3. Relative density of composites fabricated by MI1, MI2 and MIS1 procedures as a function of preform relative density.

temperature rise refers to the eradication of oxide layer on the top of the aluminum melt surface that reduces the threshold pressure of infiltration. In fact, such a temperature rise decreases the two influential parameters on the infiltration development, i.e. the surface tension of the melt and the contact angle at the ceramic–metal interface. The reduction of these two parameters, ultimately, diminishes the threshold pressure and, consequently, eases the infiltration process [6]. In addition, conducting the process in the nitrogen atmosphere at  $T > 1150\text{ }^{\circ}\text{C}$ , generates intense reactions between the Al melt and the flowing  $\text{N}_2$  gas, favoring the infiltration of aluminum melt into the pores of the SiC preform [1,11,12]. As a matter of the fact, the Al vapor at this temperature range is high enough to induce a gas phase reaction between the aluminum and nitrogen into the interstices of the porous preform, leading to the formation of AlN phase into the voids and thus culminating in the density advancement of MI2 composites. On the contrary, the composites subjected to the MIS1 procedure have undergone a slight decrease in the value of final density. Such an observation is in contrast with some publications available in the literature, according to which inserting a sintering procedure after the infiltration has been reported to be helpful in the final density increment of composites [5,23]. The reason for such an expectation can be attributed to the higher fluidity of the Al melt at this high sintering temperature that causes a smoother filling of pores by the molten metal. However, the main issue mostly emphasized in the literature, is the higher rate of Al oxidation at temperatures around  $1400\text{ }^{\circ}\text{C}$ , resulting in the formation of the Al oxide phase that displays a higher density than the pure aluminum and hence increasing the final density of composites [12,25]. To shed light on this issue, one can observe the X-ray pattern of the specimens manufactured by the MIS1 procedure depicted in Fig. 4, as a comparison with those of obtained from MI1 and MI2 regimes. As can be observed in the pattern, firing the specimen at  $1350\text{ }^{\circ}\text{C}$  in the Ar ambient has left no tangible changes in phase composition of the MIS1 sample compared to MI1. This can be associated with the neutrality of the applied Ar atmosphere, in which chemical reactions can be hardly activated and the oxide phase is not

detectable due to the sealed container and the lack of oxygen in the system. Therefore, the evaporation of Al melt at temperatures higher than  $1300\text{ }^{\circ}\text{C}$  can be the only reason that comes to mind for the mentioned slight reduction of final density in the MIS1 composites. On the other hand, the most obvious distinguishing parameter in the XRD patterns refers to the presence of the AlN phase in the pattern related to the MI2 sample. This confirms the abovementioned issue about the significance of a high infiltration temperature in formation of the AlN phase. The fact is that, through the temperature range from  $1150\text{ }^{\circ}\text{C}$  to  $1350\text{ }^{\circ}\text{C}$  and even at higher temperatures, the AlN phase can remain thermodynamically stable [26,27]. On the other hand, the absence of AlN in the microstructure of the MI1 processed sample is resulted from the application of a low infiltration temperature ( $950\text{ }^{\circ}\text{C}$ ) which is not high enough to result in the AlN formation. The other phases such as  $\text{Al}_4\text{C}_3$  and  $\text{MgAl}_2\text{O}_4$  can be, however, detected in all test specimens. What should be taken into account is that the in situ formation of interphases in the interface location of a composite is, hardly, avoidable and the mechanical properties of composites are seriously affected by characteristics of these interphases. For instance, the Al carbide phase would undoubtedly have detrimental effects on the impact energy of final composites. The spinel phase, on the other hand, is regarded as a contributive agent in manufacturing the specimens. Formation of this phase is highly depended on the consumption of free oxygen from the top of molten metal and hence reduction of the oxygen volume in the atmosphere. This finally hinders the appearance of oxide layer as a detrimental factor against the infiltration [4].

### 3.1.2. MIS2 at 1150, 1250, and 1350 °C

As can be observed in Fig. 5, contrary to those obtained from the MIS1 procedure, composites produced through the MIS2 regime at  $1150\text{ }^{\circ}\text{C}$  have revealed no signs of reduction in the value of final density, yet demonstrating a slight increment. In other words, the sintering stage after the infiltration under the  $\text{N}_2$  atmosphere has been found more successful to hit the higher values of final density than that of MI1 composites, in

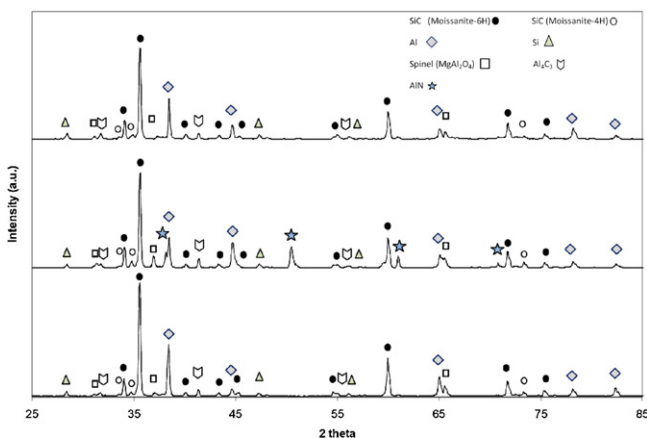


Fig. 4. The XRD pattern of composites fabricated by (a) melt infiltration at  $950\text{ }^{\circ}\text{C}$  (MI1), (b) melt infiltration at  $1350\text{ }^{\circ}\text{C}$  (MI2), and (c) melt infiltration at  $950\text{ }^{\circ}\text{C}$  followed by sintering at  $1350\text{ }^{\circ}\text{C}$  for 180 min in Ar atmosphere (MIS1).

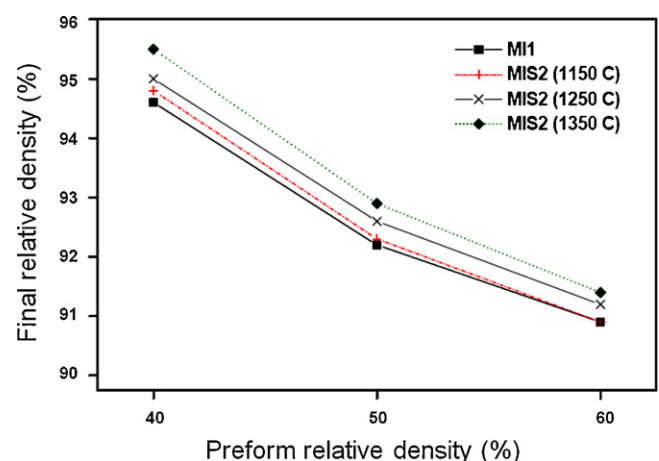


Fig. 5. Final relative density of composites fabricated by the MI1 and MIS2 (at 1150, 1250 and  $1350\text{ }^{\circ}\text{C}$ ) procedures, as a function of preform relative density.

comparison with running the sintering stage under Ar gas. However, the close values of final densities in MI1 and MIS2 composites cast a shadow on reliability of the above observation. To explore the effect of nitrogen atmosphere in this respect, the sintering stage of MIS2 was designed to be carried out at two higher temperatures of 1250 and 1350 °C, in addition to 1150 °C. The upward transition of final density graph relative to the sintering temperature of 1250 °C suggested the influence of N<sub>2</sub> gas on the enhancement of composites final density. Since a proper densification of SiC ceramics can be hardly attained at temperatures below 1600 °C, higher densities of MIS2 composites must not have been originated from the sintering of SiC particulates. Moreover, the evaporation of Aluminum melt at high temperatures can be a cause of decrease in the final density of MI2 and MIS2 produced composites, as formerly explained for MIS1 specimens. In particular, the effect of Al evaporation must be identical for all the abovementioned procedures. Therefore, another criterion must be involved and another reason must be responsible for the improvement of the final density in MI2 and MIS2 composites, compared to MI1. To shed light on this fact, XRD experiment was performed to analyze the phase structure of MIS2 specimens. As can be observed in Fig. 6, the specimens soaked at different sintering temperatures of MIS2 procedure have demonstrated AlN peaks to reveal presence of this phase in their microstructure. As mentioned before, the occurrence of a forceful reaction between the high-pressure Al gas and nitrogen at higher temperatures than 1150 °C, gave rise to the intense formation of AlN phase in the porosities and interstices of the processed specimen. Such a scenario was, previously, found to be in charge for the enhancement of final density in the MI2 produced composites, as well. The more obvious and higher AlN peak intensities concerning with the samples sintered at 1250 °C, implies formation of the higher fractions of AlN phase at this temperature and could be a good evidence for the aforementioned upward transition of final density in Fig. 5. In order to have a proof for the presence of AlN phase in the microstructure of the MIS2 composites at 1250 °C, SEM figures were obtained from an interstice of the specimen,

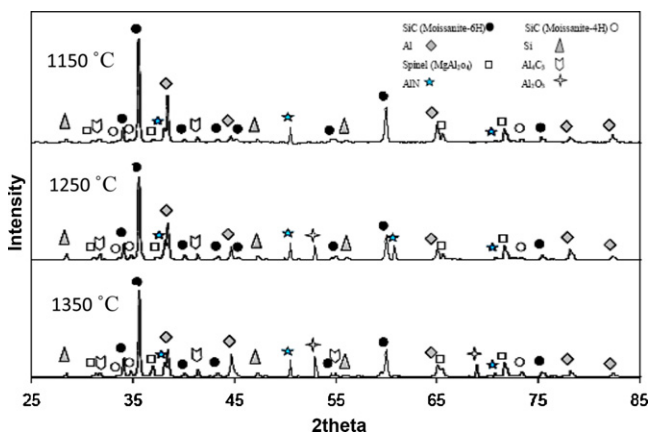


Fig. 6. The XRD pattern of composites fabricated by melt infiltration at 950 °C and sintering at (a) 1150 °C, (b) 1250 °C, and (c) 1350 °C for 180 min in N<sub>2</sub> atmosphere (MIS2).

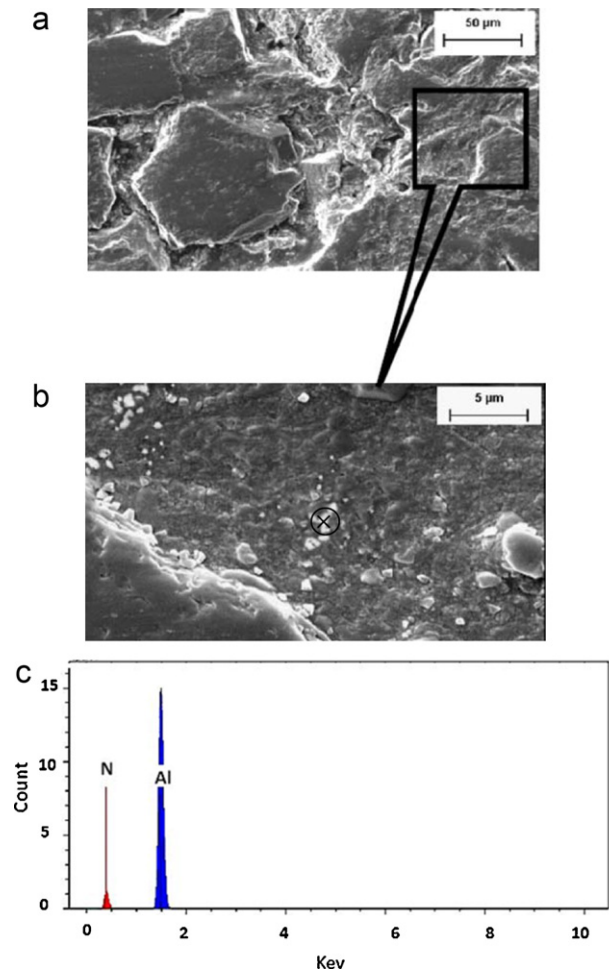


Fig. 7. (a) Composite microstructure fabricated by the infiltration at 950 °C, followed by sintering at 1250 °C in N<sub>2</sub> atmosphere for 3 h (MIS2, 1250 °C), (b) magnified micrograph from the circled interstice in Fig. 6(a), in which AlN has been formed and (c) energy dispersive spectroscopy (EDS) pattern from the crossed point in Fig. 6(b).

determined by a rectangular in Fig. 7(a). A magnified view from the labeled position of the above SEM micrograph can be seen in Fig. 7(b) and energy dispersive spectroscopy (EDS) analysis (Fig. 7(c)) was developed from the interstice and crossed locations on the SEM micrograph of Fig. 7(b). The conspicuous peaks confirming the existence of Al and N in the signed positions support this theory that improvement in the final density of MIS2 composites could be attained in the light of intense reaction between aluminum and nitrogen in the voids of the porous preform.

The abnormal upper shift of the final density graph at 1350 °C (Fig. 5), on the other hand, can be hardly justified by the above theory. Indeed, formation of the aluminum nitride phase at this temperature must be contributive to enhance final densities, based on the above discussion, but the mentioned shift can be hardly taken in granted. Yet the sintered specimens at 1350 °C have experienced more than 0.9% rise in the value of density. As can be seen in the XRD graph of Fig. 6, presence of free oxygen in the sintering atmosphere of these composites (at 1350 °C) has resulted in the formation of Al oxide phase. This

might have been generated by deficiencies in the sealing system of the set-up during this test and consequently penetration of the oxygen gas in the furnace. Bearing in mind that Al oxide phase, generally, displays a higher density compared to AlN, existence of such a phase in the microstructure of these composites (sintered at 1350 °C) must be the underlying reason for their higher values of final densities.

### 3.2. Impact resistance

To explore the effect of different processing methods on the impact behavior of the composites, the specimens were subjected to the impact energy experiment. Fig. 8 represents a comparison between the aforementioned fabrication methods in terms of the impact resistance values. Due to the sensitivity of mechanical properties from the amount of relative density, the manufacturing processes were designed to result in the specimens with the closest values of final densities. As a result, the relative density of the composites has also been added on the graphs relative to each method. As can be observed in figure, higher final density of composites processed by MI2 has led to the higher values of impact energy rather than those fabricated by MI1. However, the very interesting feature, inferred from figure, is the superiority of impact energy in the MIS produced composites, contrary to their lower relative density compared to the infiltrated ones. To shed light on this consequence, SEM figures (Fig. 9) were provided from the interface position of the abovementioned different kinds of composites. The well-known fact is that the mechanical properties of a composite can be seriously changed by the quality of interfaces in these materials. The interface formation, on the other hand, is highly dependent on the diffusive mechanisms, the activation of which requires prolonged times and high temperatures. Accordingly, the added sintering procedure (1350 °C for 3 h) exerted to the MIS produced composites, plays a contributive role for the activation of

diffusive mechanisms and thus, results in a convenient interface formation between SiC and aluminum [28]. Fig. 9 confirms the accuracy of this issue by showing the SEM figures concerning with the interface of manufactured composites. Moreover, the higher density of MIS2 composites, contrary to the expectations, has not ended in a superior impact resistance, compared to the MIS1 samples. It must have been originated from the presence of brittle AlN and Al<sub>2</sub>O<sub>3</sub> phases in the microstructure of these specimens, as previously discussed. On the other hand,

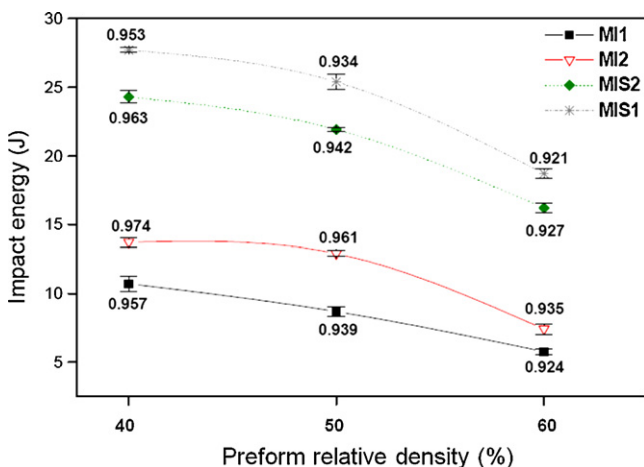


Fig. 8. Impact energy of the composites fabricated by (a) melt infiltration at 950 °C (MI1), (b) melt infiltration at 1350 °C (MI2), (c) melt infiltration at 950 °C followed by sintering at 1350 °C for 180 min in Ar atmosphere (MIS1), and (d) melt infiltration at 950 °C followed by sintering at 1350 °C for 180 min in N<sub>2</sub> atmosphere (MIS2).

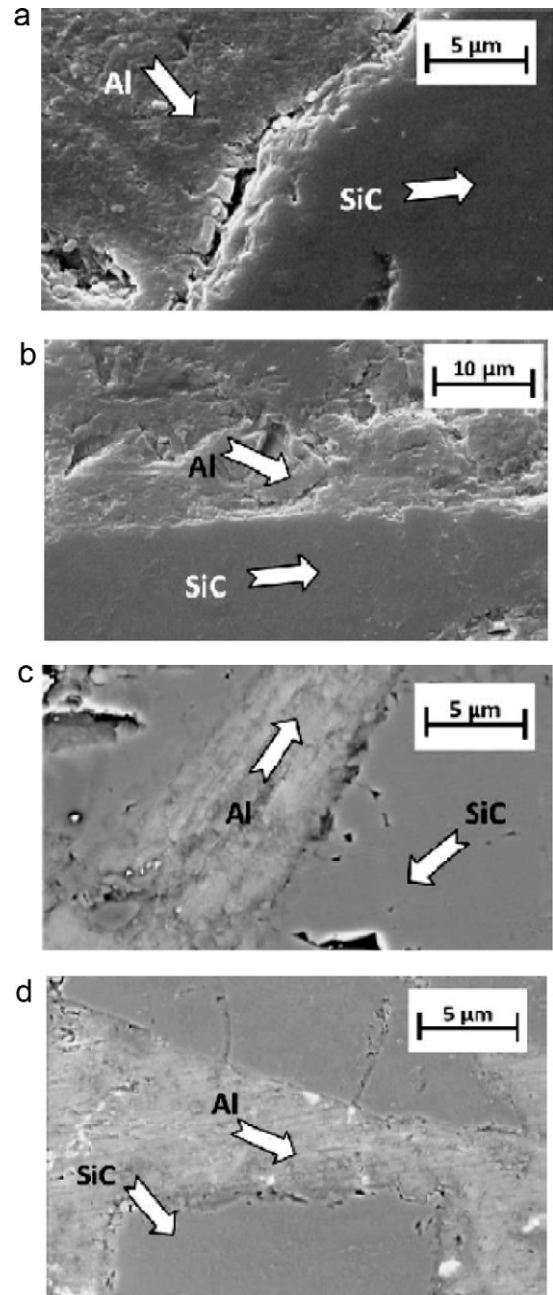


Fig. 9. Scanning electron micrographs (SEM) concerning with the interface of composites fabricated by (a) melt infiltration at 950 °C (MI1), (b) melt infiltration at 1350 °C (MI2), (c) melt infiltration at 950 °C followed by sintering at 1350 °C for 180 min in Ar atmosphere (MIS1), and (d) melt infiltration at 950 °C followed by sintering at 1350 °C for 180 min in N<sub>2</sub> atmosphere (MIS2).

the ascending trend of impact energy in return of the reduction in initial density of SiC preforms, can be interpreted by the increment in the fraction of tough aluminum phase that naturally leads to the highest impact energy for the composites fabricated based on the 0.4 TD preforms.

#### 4. Conclusions

Final relative density and impact behavior of the melt infiltrated Al/SiC composites have been studied, in the present investigation, through the application of four variable processing conditions, named MI1, MI2, MIS1 and MIS2.

The most substantial conclusions can be outlined as below:

- (1) Composites fabricated by the MI2 procedure have represented the highest values of final density among all other examined methods. Presence of the AlN phase in the microstructure of these composites implies the occurrence of an intense reaction between the Al melt and nitrogen atmosphere in the interstices of the porous preform. It also, demonstrates the most significant effect on the enhancement of final density of the composites sintered in nitrogen after the infiltration stage (MIS2), compared to MI1 produced ones.
- (2) The additional sintering stage, under the argon atmosphere, results in a moderate decline in the final density of MIS1 produced composites after the infiltration. This must have been caused by the evaporation of aluminum through soaking the specimens at the sintering temperature.
- (3) Superior impact resistance of MIS composites, compared to MI ones must be attributed to the convenient interface formation in these materials. While formation of the interface in composites is highly depended on the diffusive mechanisms, the sintering stage after the infiltration provides extended time and high temperatures for the activation of these mechanisms.
- (4) The lower impact energy of MIS2 composites in comparison with their MIS1 counterparts can be only originated from the presence of the brittle AlN phase in their microstructure.

#### Acknowledgements

The authors of the present article would like to express their profound gratitude to Prof. R. Emadi, Mr. M. Haghightzadeh

and Mr. M.G. Haghighi for their valuable comments and helpful cooperation during the course of this research.

#### References

- [1] M.I. Pech-Canul, M.M. Makhlof, *J. Mater. Synth. Process.* 8 (2000) 35–53.
- [2] C. Garcia-Cordovilla, E. Louis, J. Narciso, *Acta Metall.* 47 (1999) 4461–4479.
- [3] G.P. Martins, D.L. Olson, G.R. Edwards, *Metall. Mater. Trans. B* 19B (1988) 95–103.
- [4] A. Zulfia, R.J. Hand, *J. Mater. Sci.* 37 (2002) 961–995.
- [5] E. Ahlatci, E. Candan, H. Cimenoglu, *Metall. Mater. Trans. A* 35A (2003) 2127–2141.
- [6] J. Tian, E. Pinero, H. Narciso, E. Louis, *Scripta Mater.* 53 (2005) 1483–1488.
- [7] E. Candan, H.V. Atkinson, H. Jones, *J. Mater. Sci.* 35 (2000) 4955–4960.
- [8] E. Candan, H.V. Atkinson, H. Jones, *J. Mater. Sci.* 32 (2000) 289–294.
- [9] E. Candan, *Mater. Lett.* 60 (2006) 1204–1208.
- [10] E. Candan, H.V. Atkinson, H. Jones, *Scripta Mater.* 38 (1998) 999–1002.
- [11] M.I. Pech-Canul, R.N. Katz, M.M. Makhlof, *J. Mater. Process. Technol.* 108 (2000) 68–77.
- [12] F. Ortega-Celaya, M.I. Pech-Canul, M.A. Pech-Canul, *J. Mater. Process. Technol.* 183 (2007) 368–373.
- [13] B.C. Pai, G. Ramani, R.M. Pillai, K.G. Satyanarayana, *J. Mater. Sci.* 30 (1995) 1903–1910.
- [14] M.I. Pech-Canul, R.N. Katz, M.M. Makhlof, *Metall. Mater. Trans. A* 31A (2000) 565–573.
- [15] K.B. Lee, H.S. Sim, S.H. Kim, K.H. Han, H. Kwon, *J. Mater. Sci.* 36 (2001) 3179–3188.
- [16] K. Aoki, O. Izumi, *Nipp. Kinz. Gakk.* 43 (1979) 1190–1196.
- [17] C.T. Lui, C.L. White, J.A. Horton, *Acta Metall.* 33 (1985) 213–229.
- [18] K.P. Plucknett, P.F. Becher, K.B. Alexander, *J. Microsc.* 185 (1997) 206–216.
- [19] K.P. Plucknett, P.F. Becher, R. Subramanian, *J. Mater. Res.* 12 (1997) 2515–2517.
- [20] R. Subramanian, J.H. Schneibel, K.B. Alexander, K.P. Plucknett, *Scripta Mater.* 35 (1996) 583–588.
- [21] P. Plucknett, T.N. Tiegs, P.F. Becher, U.S. Pat. No. 5,905,937 (May 18, 1999).
- [22] P. Plucknett, T.N. Tiegs, P.F. Becher, S.B. Waters, P.A. Menchhofer, *Ceram. Eng. Sci. Process.* 17 (1996) 314–321.
- [23] K.P. Plucknett, P.F. Becher, *J. Am. Ceram. Soc.* 84 (2001) 55–61.
- [24] A.M. Zahedi, H.R. Rezaie, J. Javadpour, Mehdi Mazaheri, M.G. Haghighi, *Ceram. Int.* 35 (2009) 685–691.
- [25] K.P. Plucknett, P.F. Becher, S.B. Waters, *J. Am. Ceram. Soc.* 81 (1998) 1839–1844.
- [26] Q. Zheng, R.G. Reddy, *J. Mater. Sci.* 39 (2004) 141–149.
- [27] Q. Zheng, R.G. Reddy, *Metall. Mater. Trans. B* 34B (2003) 793–804.
- [28] B.S. Murty, S.K. Thakur, B.K. Dhindaw, *Metall. Mater. Trans. A* 31A (2000) 319–325.